Topological *p-n* junction

Jing Wang,[1,2,3] Xi Chen,[3] Bang-Fen Zhu,[1,3] and Shou-Cheng Zhang[1,2]
[1]*The Institute of Advanced Study, Tsinghua University, Beijing 100084, China*
[2]*Department of Physics, Stanford University, Stanford, California 94305-4045, USA*
[3]*State Key Laboratory of Low-Dimensional Quantum Physics and Department of Physics, Tsinghua University, Beijing 100084, China*
(Received 8 February 2012; revised manuscript received 7 June 2012; published 19 June 2012)

We consider a junction between surface p type and surface n type on an ideal topological insulator in which carrier type and density in two adjacent regions are locally controlled by composition graded doping or electrical gating. Such junction setting on topological insulators are fundamental for possible device application. A single gapless chiral edge state localized along the junction interface appears in the presence of an external magnetic field, and it can be probed by scanning tunneling microscopy and transport measurements. We propose to realize this topological *p-n* junction in $(Bi_{1-x}Sb_x)_2Te_3$, which has insulating bulk properties and a tunable surface state across the Dirac cone.

DOI: 10.1103/PhysRevB.85.235131 PACS number(s): 73.20.−r, 68.37.Ef, 73.40.Lq, 73.43.Cd

I. INTRODUCTION

Topological insulators are new states of quantum matter with a full insulating gap in the bulk and gapless edge or surface states interesting for condensed-matter physics.[1–4] The surface states of a three-dimensional (3D) topological insulator are comprised of an odd number of massless Dirac cones with spin-helical structure in the momentum space which are protected by time-reversal symmetry. Such spin-helical metallic surface states are expected to host a wide range of exotic quantum phenomena such as Majorana fermions,[5] image magnetic monopole,[6] and topological magnetoelectric effect.[7] The single Dirac cone on the Bi_2X_3 (X = Se and Te) surface[8–10] can be viewed as 1/4 of graphene,[11] and it is predicted to exhibit half-integer quantum Hall effect,[7] which is a unique property of a time-reversal symmetry-breaking surface and is determined by the bulk topology. Extensive efforts such as chemical doping and electric gating have been made to achieve the purely conducting surface in transport on topological insulators,[12–19] however, they are hindered by intrinsic defects in the materials where Bi_2X_3 is the significant bulk conduction.

Recently, three experimental groups have successfully engineered the band structure of topological insulators by molecular beam epitaxy growth of $(Bi_{1-x}Sb_x)_2Te_3$ (Refs. 20 and 21) ternary compounds and tetradymite $Bi_{2-x}Sb_xTe_{3-y}Se_y$.[22] By tuning the ratio of bismuth to antimony, they can get ideal topological insulators with truly insulating bulk and tunable surface state across the Dirac cone (p to n type) that behave like 1/4 of graphene. By composition graded doping one may form a *p-n* junction (PNJ) on a topological insulator surface (see Fig. 1), which is similar to graphene PNJ.[23–25] The properties in such a junction setting of topological insulators are not yet known.[26] On the other hand, graphene PNJs are not only promising for transistors, but are also predicted to host novel phenomena reflecting the massless Dirac character of carriers such as Klein tunneling[27] and Veselago lensing.[28] Therefore, it is important and straightforward to study the physics and relevant applications of PNJ on a topological insulator surface in analogy of graphene junction. The topological insulator surface junction is also different from the graphene junction for it only consists of a single Dirac cone. If a magnetic field is applied perpendicular to the surface junction, the different types of carriers would give rise to a quantized Hall conductance $\pm e^2/2h$ in the n and p regions, respectively, so that a single chiral edge state arises along the *p-n* interface. In the following, we will refer to such a PNJ on a topological insulator surface as a "topological *p-n* junction." The gapless chiral edge mode localized at the PNJ can be controlled by gating and magnetic field, which may be probed through scanning tunneling microscopy (STM) and transport measurements. The theoretical work here may serve a purpose in motivating experimentalists to fabricate such a device for applications of topological insulators.

The organization of this paper is as follows. After this introductory section, Sec. II describes two theoretical proposals for fabricating the topological *p-n* junction. Section III describes the model and results for the topological *p-n* junction when applying a perpendicular magnetic field. Section IV discusses the experimental methods to measure such chiral edge state. Section VI concludes this paper.

II. THEORETICAL PROPOSALS

We propose two methods to fabricate the topological *p-n* junction. One is composition graded doping, the other is electrostatic gating. The compound $(Bi_{1-x}Sb_x)_2Te_3$ with x = 0.94 (0.96) is an ideal topological insulator with surface n (p) doping, where the surface Dirac cone is in the insulating bulk gap and the Fermi level stays slightly above (below) the Dirac cone.[20] In analogy to the growth method of PNJ in *p*-GaAs/*n*-$Al_xGa_{1-x}As$, one can fabricate the junction between p-type and n-type topological insulators by composition graded doping from x = 0.94 to x = 0.96 to achieve spatially variable Dirac cone structures [Fig. 1(a)]. While in electrostatic gating, one can use the global back gate to control the position of surface Dirac cone in the bulk gap, combined with the local top gate to control density and carrier type locally [Fig. 1(b)]. This will result in device configurations with adjacent n-type and p-type regions on the top surface (in general, the top surface and bottom surface are not exactly the same due to the substrate, therefore a PNJ could be realized only on the top surface by doping and gating, while the bottom surface is just p or n doped), separated by an electrically tunable PNJ,

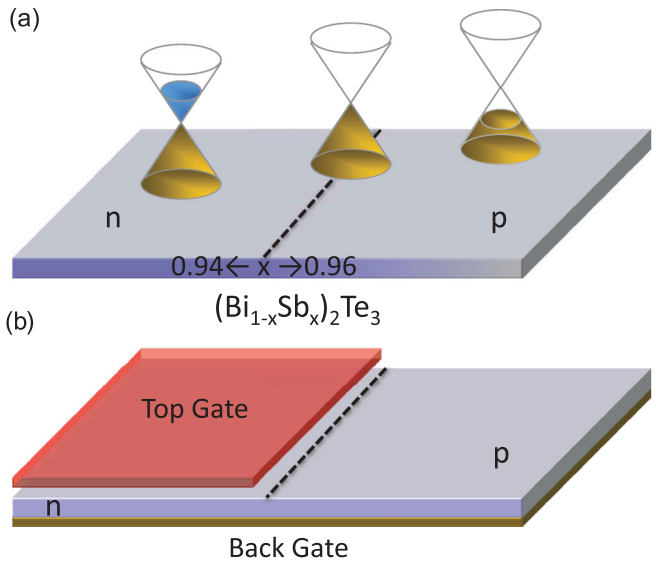

FIG. 1. (Color online) The schematic of the topological p-n junction grown by doping of topological insulator alloys $(Bi_{1-x}Sb_x)_2Te_3$. (a) Compositionally graded doping to achieve spatially variable Dirac cone structure. (b) Electrostatic gating with back gate and top gate to locally control density and carrier type.

very similar to graphene PNJ.[23] Different from the gating in graphene PNJ, here the capability of the top gate to control the carrier type and density is limited, therefore it is better to start from $(Bi_{1-x}Sb_x)_2Te_3$ with $x = 0.96$ rather than Bi_2Te_3 or Sb_2Te_3. The Fermi velocity of the Dirac electron in the p and n regions of such a topological p-n junction are almost the same.[20]

The thickness of the depletion layer of the junction at zero bias can be estimated through Poisson equation

$$\frac{d^2V(x)}{dx^2} = -\frac{\rho(x)}{\epsilon}, \tag{1}$$

where ϵ is the dielectric constant, $V(x)$ is the electric potential, and ρ is the carrier density. With the condition that there are no free carriers in the depletion area and charge neutrality, one can get the relation between the thickness of depletion layer l and the potential barrier V_d,

$$l = \sqrt{\frac{2\varepsilon(p+n)V_d\delta}{enp}}. \tag{2}$$

Here n (p) is the surface electron (hole) density and δ is the penetration depth of the surface state inside the sample. With $\delta \sim 1$ nm, $\varepsilon \sim 100$, $eV_d \sim 40$ meV, and $n \sim p \approx 1 \times 10^{12}$ cm^{-2}, the thickness of the topological p-n junction is estimated to be $l \sim 9.4$ nm.

III. MODEL AND RESULTS

The effective model[8,29] describing the massless two-dimensional (2D) Dirac fermion of a topological p-n junction reads

$$\mathcal{H} = v_F(\hat{\mathbf{z}} \times \boldsymbol{\sigma}) \cdot \mathbf{k} + U(x), \tag{3}$$

where v_F is the Fermi velocity, $\boldsymbol{\sigma} = (\sigma_1,\sigma_2,\sigma_3)$ are Pauli matrices that act on the electron spin degrees of freedom, $\mathbf{k} = -i\nabla$ is the canonical momentum operator on the surface (x-y plane), we set $\hbar \equiv 1$, $U(x)$ is the electrostatic potential step at the p-n interface, which can be modeled as $U(x) = [\tanh(2x/l) + 1]\Delta/2$, and Δ is just the Fermi energy difference between the p and n regions [see Fig. 2(a)]. On such junction setting, due to the suppressed backscattering on the topological insulator surface, the interference between the incident and reflected waves will result in a standing-wave pattern on the surface which decays faster than a conventional 2D electron gas, and has been observed by STM experimentally.[30]

More interestingly, when a perpendicular magnetic field $\mathbf{B} = B\hat{z}$ is applied to the junction, a gapless chiral edge state may appear along the interface in the quantum Hall regime. The basic picture of the formation of a chiral edge state along the PNJ is easily visualized as skipping orbital semiclassically, the change in sign of charge carriers across the PNJ produces a change in the direction of the Lorentz force, causing classical trajectories to curve back towards the interface from both sides. The orbital effect of magnetic field can be obtained by Peierls substitution $\mathbf{k} \to \mathbf{k} + e\mathbf{A}$ in Eq. (3), where $\mathbf{A} = (0, Bx, 0)$ is the vector potential. Here we choose the Landau gauge, thus $\mathbf{A}$ is parallel to the PNJ and vanishes at the interface, and the canonical momentum k along the y axis is a good quantum number. The energy spectrum for the PNJ is plotted in Fig. 2(b) with $l = l_m$ (the magnetic length $l_m \sim \sqrt{\hbar/eB} \sim 10$ nm at 11 T). The Fermi level intersects with only one chiral channel of mixed electron-hole character with linear dispersion (blue curve), where the electronlike channel is from the n region and the holelike channel is from the p region; both of them are from the nondegenerate zero mode of Landau levels (LLs) and contribute to $\pm e^2/2h$ Hall conductance. The density of the chiral edge state is shown in Fig. 2(c), which is indeed the edge mode confined along the PNJ. The scale of such chiral edge state is about 10 nm, which is smooth on the scale of l_m. To see the chiral edge state more clearly we consider an abrupt potential step, and in order to simplify the notation, we measure energies in units of $\hbar v_F/l_m$ and lengths in units of l_m. Eigenstates of Eq. (3) with magnetic fields that decay for $x \to \infty$ have the form[31]

$$\Psi(x,y) = e^{iky}\Phi(x+k), \tag{4}$$

$$\Phi_n(\xi) = e^{-(1/2)\xi^2}\begin{pmatrix} \varepsilon H_{\varepsilon^2/2-1}(\xi) \\ H_{\varepsilon^2/2}(\xi) \end{pmatrix}, \tag{5}$$

$$\Phi_p(\xi) = e^{-(1/2)\xi^2}\begin{pmatrix} (\varepsilon-\Delta) H_{(\varepsilon-\Delta)^2/2-1}(\xi) \\ H_{(\varepsilon-\Delta)^2/2}(\xi) \end{pmatrix}. \tag{6}$$

Here $H_\alpha(x)$ is the Hermite function. The dispersion relation between energy ε and momentum k follows by substitution of state (4) into the boundary condition $\Psi_n(0,y) = \Psi_p(0,y)$, and particle current conservation $\Psi_n^\dagger(0,y)\sigma_y\Psi_n(0,y) = \Psi_p^\dagger(0,y)\sigma_y\Psi_p(0,y)$. Thus we obtain

$$e^{-(k^2/2)}\begin{pmatrix} \varepsilon H_{\varepsilon^2/2-1}(k) \\ H_{\varepsilon^2/2}(k) \end{pmatrix} = e^{-(k^2/2)}\begin{pmatrix} (\varepsilon-\Delta) H_{(\varepsilon-\Delta)^2/2-1}(k) \\ H_{(\varepsilon-\Delta)^2/2}(k) \end{pmatrix}. \tag{7}$$

The numerical solution of Eq. (7) is qualitatively similar to Fig. 2(b). For $k \to -\infty$, the LLs energy in the n region

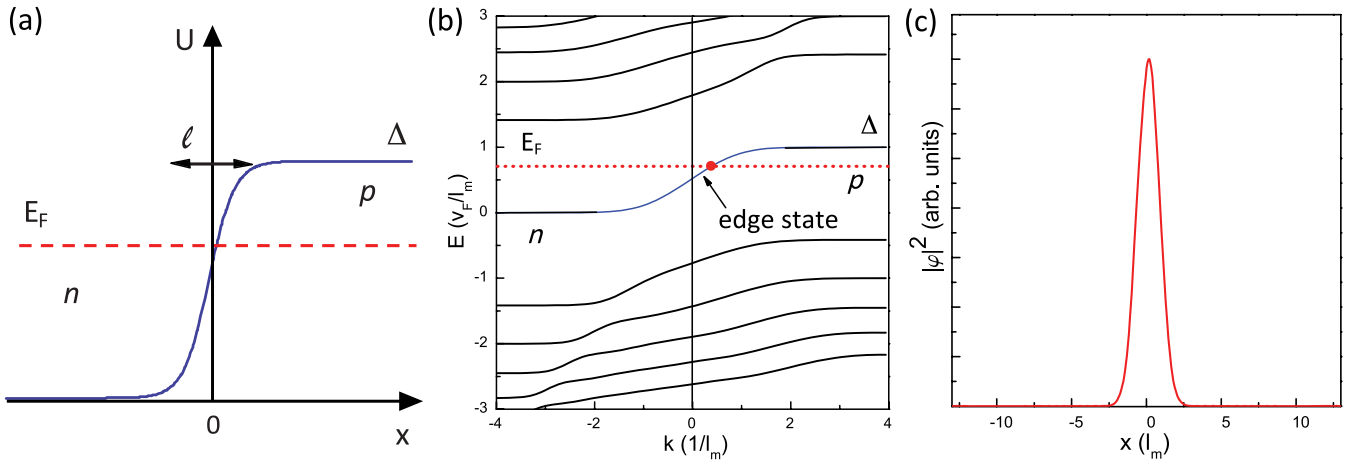

FIG. 2. (Color online) (a) Potential step at the PNJ. The electrostatic potential $U(x)$ increases from 0 to Δ over a distance l around $x = 0$. The Fermi level E_F lies in the conduction band in the n-doped regime and in the valence band for the p-doped regime. (b) Energy spectrum at the PNJ. The blue line denotes the gapless chiral edge state confined along the p-n interface, where the density of the edge state around E_F is plotted in (c). The flat bands at finite k are just the LLs in the n and p regions.

are at $\varepsilon_N^2/2 = N$, which is $\varepsilon_N = \pm\sqrt{2}(\hbar v/l_m)\sqrt{N}$, while for $k \to +\infty$ the energy is $(\varepsilon_N - \Delta)^2/2 = N$, which is $\varepsilon_N = \pm\sqrt{2}(\hbar v/l_m)\sqrt{N} + \Delta$, and the velocity $v_N = \hbar^{-1} d\varepsilon_N/dk$ vanishes. Those flat bands at finite k in Fig. 2(b) are LLs in the n and p regions. The chiral edge state does not exist if the potential barrier is too high, in which case the p and n regions are independent, and the edge channels from both sides cannot couple to each other due to energy mismatch. From Eq. (7), the chiral edge state with $0 < \varepsilon < \Delta$ around $k = 0$ exists only when $\varepsilon^2/2 - 1 < 0$ and $(\varepsilon - \Delta)^2/2 - 1 < 0$, which gives the criterion

$$\Delta < 2v_F\sqrt{2eB\hbar}, \tag{8}$$

where the right part is just the energy difference between the second LL and zero mode. This reflects that increasing the electric field across the junction via gate voltages will destabilize the edge modes. With $\Delta = 40$ meV, the magnetic field B must be greater than 2.0 T in order for such edge states to exist.

IV. DISCUSSION

We now propose a practical way to detect such chiral edge states [see Fig. 3(a)]. The state localized at the junction on a topological insulator surface can be imaged by STM. By applying a magnetic field, the LL structure of surface states is formed and has already been observed by STM.[32,33] Discrete LLs appear as a series of peaks in the differential conductance spectrum (dI/dV), and the dependence of the LLs on the magnetic field B shows that the energy of the LLs is proportional to $\mathrm{sgn}(N)\sqrt{|N|B}$, where N is the LL index. The energy of zero mode $N = 0$ in the p and n regions can be measured, between which there are no states in either region, as shown in Fig. 3(b). Then by moving the STM tip to the PNJ area, one should observe a peak in the dI/dV spectrum with energy between zero mode in the p and n regions, and this should be the manifestation of the chiral edge mode. Moreover, the formation of the chiral edge mode takes place at $B > B_\star = \Delta^2/8e\hbar v_F^2$; therefore such peak will disappear in the dI/dV spectrum when decreasing the magnetic field.

In addition to the above surface-sensitive technique, one can employ transport measurements. Instead of measuring the Hall conductance, we can directly measure the longitudinal resistance R along the PNJ. In a conventional junction, there is no conducting channel along the PNJ. However, in the quantum Hall regime, the single chiral edge mode along the topological p-n junction will contribute to transport. As shown in Fig. 3(c), R is measured *along* the PNJ, with current source at 1, ground at 2, and voltage measured between 3 and 4; we will get the

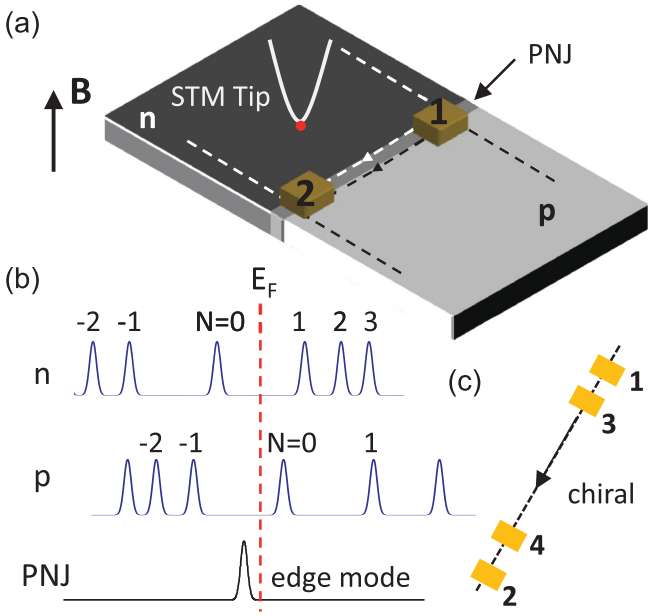

FIG. 3. (Color online) (a) Setup for measuring the gapless chiral edge state along the PNJ. (b) Schematic of STM measurement; the energy of chiral mode is between the zero mode in the n and p regions. (c) Schematic of the chiral mode along the p-n interface and transport measurement.

longitudinal resistance $R = h/e^2$ contributed from the chiral edge channel. Backscattering is forbidden along this channel, therefore by reversing the current flow at 1 and 2, R will approach infinity. Besides this, when the magnetic field is smaller than the critial value $B_\star$, such chiral edge channel will disappear, and we will get zero conductance.

Finally, we would like to discuss the possibility of longitudinal conductance plateaus in our setup. The edge current of the interface state will flow into side surfaces, and both the top and bottom surfaces will contribute to the side surface currents. In our setup where the top surface is in the ambipolar regime and the bottom surface is in the unipolar regime, the total side surface currents will become unipolar, and it will give rise to quantized longitudinal conductance as in the unipolar graphene PNJ.[23,24]

V. CONCLUSION

In summary, we propose to use composition graded doping and electric gating in topological insulator alloys $(Bi_{1-x}Sb_x)_2Te_3$ to fabricate the topological p-n junction, where a single 2D Dirac cone junction on a topological insulator surface may be achieved. A single gapless chiral edge state localized along the p-n interface appears in the presence of an external magnetic field, which can be controlled by the gating and magnetic field. The edge mode can be imaged by STM as well as transport measurements. The theoretical work here may serve a purpose in motivating experimentalists to fabricate such a device, which would lead to novel designs for optoelectronics applications.

ACKNOWLEDGMENTS

We are grateful to X. L. Qi and Y. Y. Wang for insightful discussion. This work is supported by the Department of Energy, Office of Basic Energy Sciences, Division of Materials Sciences and Engineering, under Contract No. DE-AC02-76SF00515. J.W. is partly supported by the Program of Basic Research Development of China Grant No. 2011CB921901 and NSFC Grant No. 11074143.

[1] X. L. Qi and S. C. Zhang, Phys. Today **63**(1), 33 (2010).
[2] J. E. Moore, Nature (London) **464**, 194 (2010).
[3] M. Z. Hasan and C. L. Kane, Rev. Mod. Phys. **82**, 3045 (2010).
[4] X. L. Qi and S. C. Zhang, Rev. Mod. Phys. **83**, 1057 (2011).
[5] L. Fu and C. L. Kane, Phys. Rev. Lett. **100**, 096407 (2008).
[6] X. L. Qi, R. Li, J. Zang, and S. C. Zhang, Science **323**, 1184 (2009).
[7] X. L. Qi, T. L. Hughes, and S. C. Zhang, Phys. Rev. B **78**, 195424 (2008).
[8] H. Zhang, C.-X. Liu, X.-L. Qi, X. Dai, Z. Fang, and S.-C. Zhang, Nat. Phys. **5**, 438 (2009).
[9] Y. Xia, D. Qian, D. Hsieh, L. Wray, A. Pal, H. Lin, A. Bansil, D. Grauer, Y. S. Hor, R. J. Cava, and M. Z. Hasan, Nat. Phys. **5**, 398 (2009).
[10] Y. L. Chen, J. G. Analytis, J.-H. Chu, Z. K. Liu, S.-K. Mo, X. L. Qi, H. J. Zhang, D. H. Lu, X. Dai, Z. Fang, S. C. Zhang, I. R. Fisher, Z. Hussain, and Z.-X. Shen, Science **325**, 178 (2009).
[11] K. S. Novoselov, A. K. Geim, S. V. Morozov, D. Jiang, M. I. Katsnelson, I. V. Grigorieva, S. V. Dubonos, and A. A. Firsov, Nature (London) **438**, 197 (2005) .
[12] D. Hsieh, Y. Xia, D. Qian, L. Wray, J. H. Dil, F. Meier, J. Osterwalder, L. Patthey, J. G. Checkelsky, N. P. Ong, A. V. Fedorov, H. Lin, A. Bansil, D. Grauer, Y. S. Hor, R. J. Cava, and M. Z. Hasan, Nature (London) **460**, 1101 (2009).
[13] J. G. Checkelsky, Y. S. Hor, M.-H. Liu, D.-X. Qu, R. J. Cava, and N. P. Ong, Phys. Rev. Lett. **103**, 246601 (2009).
[14] J. G. Analytis, R. D. McDonald, S. C. Riggs, J.-H. Chu, G. S. Boebinger, and I. R. Fisher, Nat. Phys. **6**, 960 (2010).
[15] D. X. Qu, Y. S. Hor, J. Xiong, R. J. Cava, and N. P. Ong, Science **329**, 821 (2010).
[16] J. Chen, H. J. Qin, F. Yang, J. Liu, T. Guan, F. M. Qu, G. H. Zhang, J. R. Shi, X. C. Xie, C. L. Yang, K. H. Wu, Y. Q. Li, and L. Lu, Phys. Rev. Lett. **105**, 176602 (2010).
[17] J. G. Checkelsky, Y. S. Hor, R. J. Cava, and N. P. Ong, Phys. Rev. Lett. **106**, 196801 (2011).
[18] A. A. Taskin, Z. Ren, S. Sasaki, K. Segawa, and Y. Ando, Phys. Rev. Lett. **107**, 016801 (2011).
[19] Z. Ren, A. A. Taskin, S. Sasaki, K. Segawa, and Y. Ando, Phys. Rev. B **84**, 165311 (2011).
[20] J. Zhang, C.-Z. Chang, Z. Zhang, J. Wen, X. Feng, K. Li, M. Liu, K. He, L. Wang, X. Chen, Q.-K. Xue, X. Ma, and Y. Wang, Nature Commun. **2**, 574 (2011) .
[21] D. Kong, Y. Chen, J. J. Cha, Q. Zhang, J. G. Analytis, K. Lai, Z. Liu, S. S. Hong, K. J. Koski, S.-K. Mo, Z. Hussain, I. R. Fisher, Z.-X. Shen, and Y. Cui, Nat. Nanotechnol. **6**, 705 (2011) .
[22] T. Arakane, T. Sato, S. Souma, K. Kosaka, K. Nakayama, M. Komatsu, T. Takahashi, Z. Ren, K. Segawa, and Y. Ando, Nat. Commun. **3**, 636 (2012) .
[23] J. R. Williams, L. DiCarlo, and C. M. Marcus, Science **317**, 638 (2007).
[24] D. A. Abanin and L. S. Levitov, Science **317**, 641 (2007).
[25] B. Huard, J. A. Sulpizio, N. Stander, K. Todd, B. Yang, and D. Goldhaber-Gordon, Phys. Rev. Lett. **98**, 236803 (2007).
[26] L. A. Wray, S. Xu, M. Neupane, Y. Xia, D. Hsieh, D. Qian, A. V. Fedorov, H. Lin, S. Basak, Y. S. Hor, R. J. Cava, A. Bansil, and M. Z. Hasan, arXiv:1105.4794.
[27] M. I. Katsnelson, K. S. Novoselov, and A. K. Geim, Nat. Phys. **2**, 620 (2006).
[28] V. V. Cheianov, V. Fal'ko, and B. L. Altshuler, Science **315**, 1252 (2007).
[29] C.-X. Liu, X.-L. Qi, H. J. Zhang, X. Dai, Z. Fang, and S.-C. Zhang, Phys. Rev. B **82**, 045122 (2010).
[30] J. Wang, W. Li, P. Cheng, C. Song, T. Zhang, P. Deng, X. Chen, X. Ma, K. He, J.-F. Jia, Q.-K. Xue, and B.-F. Zhu, Phys. Rev. B **84**, 235447 (2011).
[31] A. R. Akhmerov and C. W. J. Beenakker, Phys. Rev. Lett. **98**, 157003 (2007).
[32] P. Cheng, C. Song, T. Zhang, Y. Zhang, Y. Wang, J.-F. Jia, J. Wang, Y. Wang, B.-F. Zhu, X. Chen, X. Ma, K. He, L. Wang, X. Dai, Z. Fang, X. Xie, X.-L. Qi, C.-X. Liu, S.-C. Zhang, and Q.-K. Xue, Phys. Rev. Lett. **105**, 076801 (2010).
[33] T. Hanaguri, K. Igarashi, M. Kawamura, H. Takagi, and T. Sasagawa, Phys. Rev. B **82**, 081305 (2010).